

NEAR-FIELD OPTICAL DIFFRACTION RADIATION MEASUREMENTS AT CEBAF*

P. Evtushenko[#], A. P. Freyberger, C. Y. Liu, Jefferson Lab, Newport News, VA USA
A. Lumpkin, Fermilab, Batavia, IL USA

Abstract

Optical diffraction radiation (ODR) is a promising technique, which could be used for non interceptive beam size measurements at future light sources. An ODR diagnostic station was designed and installed on a CEBAF transfer beam line. The purpose of the setup is to evaluate experimentally the applicability range for an ODR based non interceptive beam size monitor and to collect data to benchmark numerical modeling of the ODR. An extensive set of measurements were made at the electron beam energy of 4.5 GeV. The ODR measurements were made for both pulsed and CW electron beam of up to 80 μA . The wavelength dependence and polarization components of the ODR were studied using a set of insertable bandpass filters and polarizers. The typical transverse beam size during the measurements was ~ 150 microns. Complete ODR data, wavelength and polarization, were recorded for different beam sizes and intensities. The beam size was also measured with an optical transition radiation (OTR) as well as wire scanner located next to the ODR station. In this contribution we describe the experimental setup and present first results of the measurements with the comparison to the numerical simulations.

INTRODUCTION

Optical diffraction radiation is generated when a charged particle passes near a conductor at a distance comparable or smaller than $\gamma \cdot \lambda / 2\pi$, where γ is the relativistic Lorentz factor and λ is the wavelength of the radiation. The theory of the diffraction radiation is well developed [1]. In the case of a highly relativistic particle beam with large γ , a conductor located at a distance bigger than the transverse beam size will generate a significant amount of diffraction radiation in the optical wavelength range. Several ODR based schemes were suggested for non-intercepting beam size measurements [2-6]. Some of them utilize the angular distribution of the ODR whereas others make use of imaging of the radiator surface, i.e., near-field measurements. The near-field ODR was observed experimentally previously [7, 8]. A common condition in such measurements was that the integrated charge used to generate the ODR was several nC.

The Continuous Electron Beam Accelerator Facility (CEBAF) is a multipass superconducting LINAC delivering CW electron beam with an energy up to 6 GeV and average current up to 100 μA for nuclear physics

experiments on fixed targets [9]. A typical beam size in CEBAF at high energy is 100 μm . The total charge delivered by CEBAF within the time a standard video camera uses to integrate one field of a video signal (16.6 ms) and when running 100 μA beam is 1.66 μC . The combination of the these parameters, GeV range energy, 100 μm beam size and μC charge integrated within 16.6 ms, makes CEBAF an ideal facility to study develop and implement an ODR based non-intercepting beam size diagnostic, as was pointed out previously [10]. From the operational point of view it is very desirable to have such a non-intercepting beam size monitor. It can be used to detect drifts leading to a change in the betatron match early and therefore can improve beam availability for the nuclear physics experiments. A set of such beam size monitors positioned properly along a transport beam line could also provide online emittance monitoring as well as emittance measurements.

EXPERIMENTAL SETUP

The most important part of the ODR diagnostic station is the ODR radiator. The optical transition radiation (OTR) was used for reference beam size measurements. Thus we have designed and built a radiator which could be used for both OTR and ODR measurements. The radiator is shown in Fig. 1. The ODR part of the radiator is a 300 μm thin silicon wafer optically polished and aluminized on one side. The thickness of the aluminum layer is about 600 nm. The wafer is mounted on an aluminum holder in such way that its edge does not have any frame underneath. This edge of the wafer was put close to the beam to generate the ODR. Minimizing the beam scattering in the OTR screen and reducing the beam losses downstream of the radiator is always desirable.



Figure 1: ODR-OTR radiator

* Work supported by the U.S. DOE contract # DE-AC05-06OR23177

[#] Pavel.Evtushenko@jlab.org

Therefore next to the ODR radiator we have put a separate OTR radiator. The radiator is a 6 μm thin Kapton foil aluminized on one side and stretched on a frame so that it is flat. Surfaces of both radiators look as an optical mirror. The aluminization of both radiators is done to increase radiation yield.

The radiator is mounted on a stepper motor actuator with a lead screw. The actuator can position the radiator with accuracy better than 10 μm . The radiator is mounted on the actuator at an angle of 45 degrees relative to the direction of the beam propagation. Fig. 2 shows schematically the ODR diagnostic station. The setup was installed on an existing very stable girder in the beginning of the Hall-A beam line. The radiator is installed on the downstream side of the girder. An alignment laser was installed on the upstream side of the girder. The laser beam is coupled in to the beam line with the help of an insertable mirror. To set up and align the optical system, first the alignment laser was set to be at the same position and angle at the ODR radiator as the electron beam. The laser spot position would be measured on the ODR radiator itself and on a beam viewer located approximately 30 m downstream of the ODR station. Thus we could setup the angle of the alignment laser with accuracy 100 μrad relative to the beam trajectory. All optical components are mounted on two optical rails as can be seen in the Fig. 2. There are two 2" mirrors on the vertical rail to redirect the OTR and ODR light to the horizontal rail. Two 2" diameter achromatic lenses are used to image the surface of either radiator on a CCD camera. For the measurements we used a JAI-A50 CCD camera. The camera is neither cooled nor intensified. The most important feature of the camera is the signal to noise ratio (SNR) of 60 dB. There are two insertable polarizers, vertical and horizontal, installed in the optical system to study effects of polarization on the ODR measurements. There are also three motorized and remotely controlled filter wheels where band-pass and neutral density filters are installed. The video signal of the CCD camera was digitized with 10-bit frame grabber. Due to the SNR of the camera and the resolution of the frame grabber the dynamic range of our measurements was about 10^3 . There are two wire scanners installed on the same girder where the ODR diagnostic station was installed. This gave us the capability to cross check the ODR as well as OTR measurements with the wire scanners measurements.

EXPERIMENTAL RESULTS

We started our measurements by determining the beam size with the help of the OTR and the wire scanners. Unfortunately the thin Kapton OTR radiator surface happened to be somewhat misaligned with the surface of the ODR radiator. The optical system was aligned reflecting the alignment laser from the surface of the ODR radiator. As a result the OTR image from the Kapton radiator was considerably dimmer and appeared somewhat shifted. For that reason we had to use the surface of the ODR radiator for the OTR measurements.

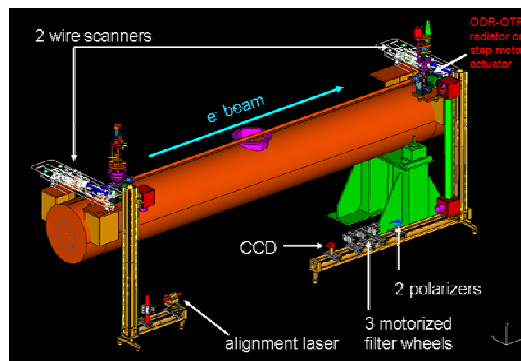


Figure 2: Schematic of ODR station

Since our goal is to develop a non-intercepting beam size measurements technique, one of the measurements we did was to change the beam size using upstream quadrupoles and measure the changes in the ODR pattern. As mentioned above the OTR and wire scanners were used to determine the beam size. We have observed that using polarizers made a difference for the measured beam size. For instance, if without polarizer we would measure the vertical and horizontal beam sizes of $\sigma_x=149 \mu\text{m}$ and $\sigma_y=157 \mu\text{m}$, then when the horizontal polarizer was inserted we have measured $\sigma_x=150 \mu\text{m}$ and $\sigma_y=130 \mu\text{m}$ and when the vertical polarizer was inserted the measurements were $\sigma_x=124 \mu\text{m}$ and $\sigma_y=160 \mu\text{m}$. That is for either polarization the beam size measured in perpendicular direction would appear to be smaller by about 20 % and the beam size measured in the direction of polarization essentially would not change. Figure 3 shows a comparison of the beam size measurements with the wire scanner, unpolarized OTR and polarized OTR for ten different quadrupole settings. The polarized OTR data are systematically much closer to the wire scanner data than the unpolarized data. At this time the polarized OTR data have much smaller statistical spread which manifests in much smoother data curves.

For the ODR measurements it is desirable to position the edge of the ODR radiator as close as possible to the beam without generating beam losses. Before inserting the ODR radiator close to the beam and running higher

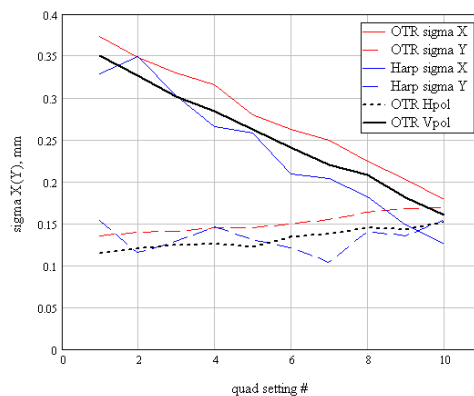


Figure 3: Cross-comparison of wire scanner and OTR data

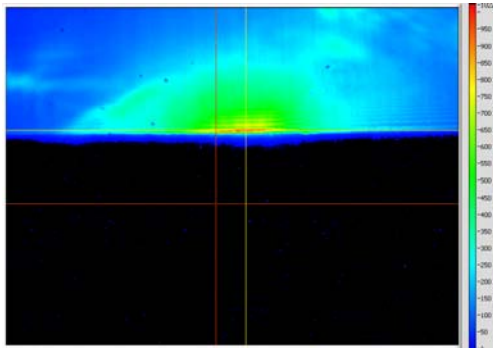


Figure 4 a: Unpolarized ODR pattern

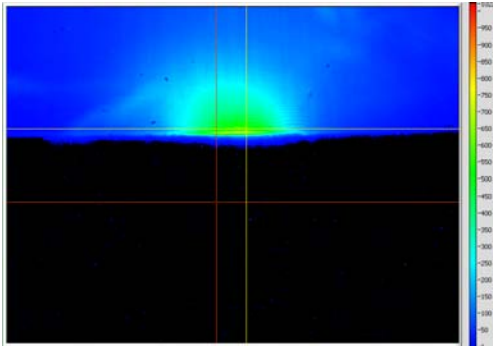


Figure 4 b: Vertically polarized ODR pattern

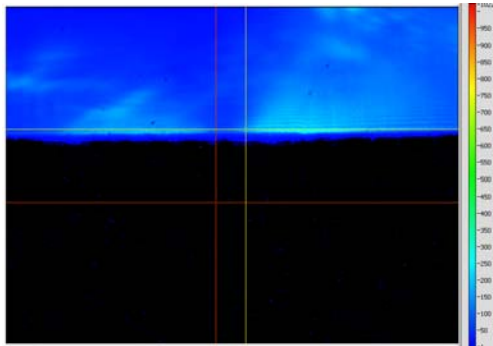


Figure 4 c: Horizontally polarized ODR pattern

current beam the vertical beam size was reduced to $110 \mu\text{m}$. The edge of the ODR radiator was positioned above the beam at 1.1 mm from the beam centroid, which is $10 \times \sigma_y$. Gradually increasing the average beam current of CW beam at $10 \mu\text{A}$ we recorded the image shown in Fig. 4 a. No beam loss was detected with the ODR radiator inserted. The field of view of the image is 6.9 mm by 5.2 mm . Note that at this beam intensity we started to saturate the CCD camera at the maximum of the intensity of the ODR pattern. The measurements are made with the beam energy of 4.5 GeV . With the vertical polarizer inserted the ODR pattern appeared to be considerably narrower (Fig. 4 b) and with the horizontal polarizer inserted we could clearly observe the double lobe pattern (Fig. 4 c). Both these observations are in agreement with the model prediction [7]. In an ODR image a small, approximately $100 \mu\text{m}$ wide, region of interest (ROI) close to the edge of

the radiator was selected. The intensity of all lines in the ROI was added and normalized to the number of lines. Using a nonlinear least square fit, a best approximation of the normalized intensity profile in the ROI by a Gaussian function was found. The sigma of the Gaussian distribution found by the fit was taken as a measure of the ODR pattern. For the previously determined ten settings of the upstream quadrupole we have measured the width of the ODR patterns without any polarizers and with vertical polarizer inserted. Results of the measurements are shown in Fig. 5 where the horizontal axis is the beam size measured via vertically polarized OTR. For both unpolarized and vertically polarized ODR data a systematic increase of the ODR pattern width is measured when the horizontal beam size is increased. The same experimental observation was made previously in [7]. Ultimately we would like to be able to use ODR for beam size measurements without any cross-calibration. As a first step towards such measurements we need to see a good agreement between the measured data and the prediction of the model. The beam size measured with the OTR and we know the distance from the beam centroid to the edge of the ODR radiator, we can calculate the expected ODR pattern distributions for these conditions. We apply then the same procedure to the model data as we did with the experimental data. The results of this would be the expected sigma of the best Gaussian fit. We did such calculations for a horizontal beam size in the range $50 \mu\text{m}$ through $350 \mu\text{m}$; the vertical beam size in the calculations was kept constant and equal to $150 \mu\text{m}$. The calculations were made for four different wavelength 450 nm , 550 nm , 650 nm and 750 nm , for unpolarized and vertically polarized ODR. The results of the calculations are shown in Fig. 5 with the results of the measurements. Note that the measurements are broadband and the calculations are narrowband. It is reasonable to assume that when the quantum efficiency of the CCD camera is taken in to account the broad band data or calculations will be somewhere in the range between 450 nm and 750 nm . Comparing the calculation and the measurements in the Fig. 5 we can conclude that the unpolarized data are in reasonable agreement with the model predictions whereas the vertically polarized data agree less with the model. However, the disagreement between the vertically polarized ODR data and the model is only about 20 %. As can be seen in Fig. 4 there is a background present in the raw ODR data. Possible sources of the background are visible synchrotron radiation and visible edge radiation from the upstream dipole, which is located only 8 m upstream of the ODR radiator. The presence of the background in the data certainly affects the results of the Gaussian fits. We consider the background to be the main reason for the discrepancy between the model prediction and the experimental results. Another set of the data was taken to study experimentally dependence of the ODR distribution on the wavelength of the radiation. Using CW electron beam with the average current, $10 \mu\text{A}$, $40 \mu\text{A}$ and $82 \mu\text{A}$, we have measured the width of the ODR distributions at 450 nm , 550 nm , 650 nm and 750 nm

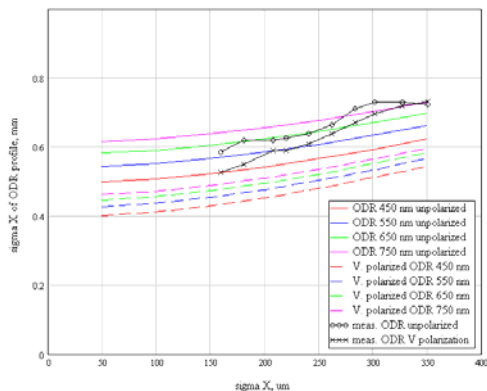


Figure 5: ODR data comparison with the model

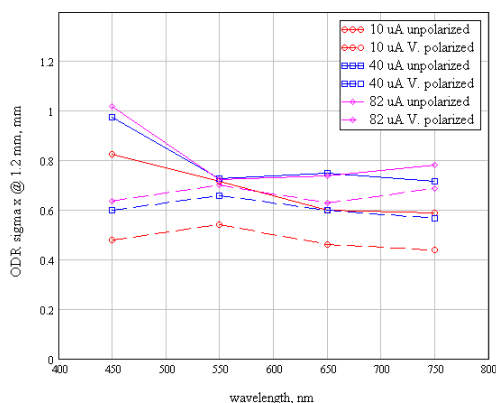


Figure 6: ODR pattern width vs. wavelength

using insertable bandpass filters with a bandwidth of 10 nm for 450 nm, 550 nm, 650 nm and 40 nm for the 750 nm. Results of the measurements are shown in Fig. 6. The first observation is that whereas the model predicts broader distributions for longer wavelengths at any distance from the beam centroid and for any beam size, as can be seen in Fig. 5, this trend does not show up in the experimental data. Here we do not provide an explanation of this observation. We are planning to examine achromaticity of the imaging optics and magnitudes of the aberrations introduced by different bandpass filters as well as make more measurements to understand the experimentally observed wavelength dependence. One more observation is that the ODR data at any wavelength, both unpolarized and vertically polarized, suggest that when the beam current was changed from 10 μA to 40 μA the beam size has changed while when the beam current was changed from 40 μA to 82 μA the beam size has not changed. Note that at the maximum CW beam average current of 82 μA (the limitation factor was the quantum efficiency of the photocathode) no measurable beam loss was observed. One can consider the fact that we could run a CW electron beam with an average current of 82 μA , have the ODR radiator 1 mm away from the beam, and not see detectable beam loss as a milestone for the ODR based diagnostics development.

When measuring the ODR patterns with the horizontal polarizer inserted we were clearly observing the double lobe distributions. However the distributions we have observed were not symmetrical as the model predicts. One possible explanation for that can be a slightly misaligned polarizer. Another cause for the asymmetry can be a background intensity distribution which is not symmetric relative to the beam position at the ODR radiator. We are planning to install one single polarizer on an insertable rotation stage and make more measurements to clarify this observation.

CONCLUSION

We have made measurements of the ODR patterns distribution using CW electron beam. The distributions were measured as a function of the beam size, wavelength and polarization. We were able to run CW beam with an average current up to 82 μA with the ODR radiator edge placed at ten times the vertical beam size without measurable beam loss. We observe significant background in the ODR data that affects the data analysis and is considered to be the main reason for the discrepancy between the model and the experiment. We are planning to improve the experimental setup to mitigate or completely eliminate the background in the ODR data.

ACKNOWLEDGMENTS

We would like to thank Lia Merminga, George Neil, Gwyn Williams and Steve Benson for stimulating and useful discussions. This work is supported by the U.S. Department of Energy under contract number DE-AC05-06OR23177.

REFERENCES

- [1] M. L. Ter-Mikaelian, High Energy Electromagnetic Processes in Condensed Media (Wiley/Interscience, New York, 1972)
- [2] D.W. Rule and R. B. Fiorito "The Use of Transition Radiation as a Diagnostic for Intense Beams", NSW Tech. Report 84-134, July 1984
- [3] D.W. Rule , R. B. Fiorito and W.D. Kimura, Proc. of BIW , 7th Workshop, AIP Conf. Proc 390 pp. 51-517 (1997)
- [4] M. Castellano, Nucl. Instrum. Methods Phys. Res., Sect. A394, 275 (1997).
- [5] A. P. Potylitsyn, Nucl. Instrum. Methods Phys. Res., Sect. B 145, 169 (1998).
- [6] P. Karataev et al., Phys. Rev. Lett. 93, 244802 (2004)
- [7] A. H. Lumpkin, W. J. Berg, N. S. Sereno, D. W. Rule, and C.-Y. Yao, Phys. Rev. ST Accel. Beams 10, 022802 (2007)
- [8] E. Chiadroni, et al., Proceedings of PAC07, Albuquerque, New Mexico, USA, p. 3982
- [9] C.R. Leeman, D.R. Douglas, and G.A. Kraft, Annu. Rev. Nucl. Part. Sci. 51, 413-50 (2001).
- [10] A. H. Lumpkin et al., Proceedings of PAC07, Albuquerque, New Mexico, USA, p. 4381